Proceedings of the 2004 IEEE
International Conference on Robotics & Automation
New Orleans, LA • April 2004

Angle-Based Methods for Mobile Robot Navigation: Reaching the Entire Plane

Kostas E. Bekris[1]
[1]Computer Science Department
Rice University
Houston, TX, 77005, USA
{bekris,kavraki}@cs.rice.edu

Antonis A. Argyros[2]
[2]Institute of Computer Science (ICS)
Foundation for Research and Technology – Hellas(FORTH)
Heraklion, Crete, Greece
argyros@ics.forth.gr

Lydia E. Kavraki[1]

Abstract— **Popular approaches for mobile robot navigation involve range information and metric maps of the workspace. For many sensors, however, such as cameras and wireless hardware, the angle between two features or beacons is easier to measure. With these sensors' features in mind, we initially present a control law, which allows a robot with an omni-directional sensor to reach a subset of the plane by monitoring the angles of only three landmarks. By analyzing the law's properties, a second law has been developed that reaches the complementary set of points. The two methods are then combined in a path planning framework that reaches any possible goal configuration in a planar obstacle-free workspace with three landmarks. The proposed framework could be used together with other techniques, such as obstacle avoidance and topological maps, to improve the efficiency of autonomous navigation. Experiments have been conducted on a robotic platform using a panoramic camera that exhibit the effectiveness and accuracy of the proposed techniques. This work provides evidence that navigational tasks can be performed using only a small number of primitive sensor cues and without the explicit computation of range information.**

Keywords: mobile robot navigation, landmarks, homing, reachability, angle-based navigation.

I. INTRODUCTION

This paper follows a minimalistic approach for mobile robot navigation. We focus on algorithms that do not use metric maps, range information or compass in order to compute a path to the goal but instead rely on angular information. The 2D version of the problem we are interested in assumes a point robot in an environment that contains three landmarks. Landmarks correspond to stationary points in the scene for which the robot can use sensor data to detect the bearing and the identity of these points relative to its orientation. The landmark coordinates, as well as the robot's position and orientation, are unknown, so triangulation [4], [3] is not possible. The goal is to guide a robot to a position for which the only known information is the difference in bearings between landmarks. In order to guarantee the visibility of landmarks the robot's sensor is assumed to be panoramic, to have infinite-radius and not to suffer from uncertainty while the environment is obstacle-free. This work is a feasibility study of angle-based control laws and our final result is that a robot is able to reach every goal configuration in a planar obstacle-free 2D three-landmark workspace, except the circle defined by the three landmarks, without any range measurements and knowledge or computation of landmark coordinates.

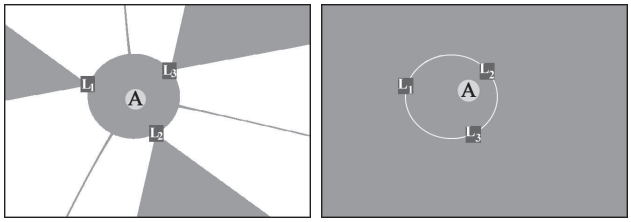

Fig. 1. Results from simulation. The robot's initial position is point A and three landmarks L_1, L_2, L_3 are visible in the scene. Every pixel could be the robot's goal, and is painted gray if it is reachable by (left) the basic control law or (right) the final framework, presented in this paper.

In order to reach the desired result we have first investigated the reachability capabilities of a simple angle-based control law by conducting extensive experiments using a simulator. The experiments showed that this control law cannot be used to move the robot on all possible points in the plane (see Fig. 1(a)). For this reason, another control law has been developed that reaches the complementary set of points. Based on geometric observations about the perceived angles, a hybrid system has been built to combine the reachability sets of the two control laws. The discrete state of the system is defined by a set of rules that selects the appropriate law for the given goal, while the continuous state is defined by the two control laws. The complete law reaches every point in the plane except from the circumscribed circle of the three landmarks (see Fig. 1(b)). Experiments with a real robot show that the proposed algorithms are able to successfully guide a robot to previsited positions with an error of a few centimeters.

The importance of this work is the validation of the argument that navigation can be achieved without solving the localization problem [7]. Combining the proposed laws with obstacle avoidance [12], [14], [21] and topological maps [8], [19] can lead to fast and reliable long-range navigation. The more powerful and complete the control law is and the lesser the requirements for its employment are, the more effective in supporting autonomous navigation the complete system will be. Moreover, the selection of angular input data makes the proposed techniques suitable to implement with vision-based and wireless sensors. Cameras do not readily provide range information. On the other hand, the calculation of image features' bearings is a trivial task, although correspondence is a difficult problem.

Correspondence, however, is trivial when wireless beacons are used. Wireless hardware has been recently proposed as a possible sensor for robotic applications [9] and there is the possibility for new wireless antennas to return the "angle of arrival" of a signal [18]. Finally, artificial landmark navigation systems can be employed without measuring the landmark coordinates during the setup phase.

There are many successful methods that achieve impressive navigational tasks after solving the scene reconstruction and localization problem, such as SLAM approaches [20], [17]. This paradigms, however, employs range data and an explicit workspace representation. On the other end of the spectrum, angle-based methods aim to guide a robot to a goal without mapping (homing). One of the first methods in this area was the "snapshot model" [5], where the current and the goal snapshots are matched with the aid of a compass and a route to the goal is computed. The same idea is prominent in the area of qualitative navigation [13]. There have been several implementations of snapshot-based techniques on real mobile robots that showed the efficiency of similar mechanisms under real-world conditions [11], [16], [7], and without the requirement of a compass [1].

In this paper, we describe the path planning framework that reaches the entire plane step by step. In Section II, we present the basic control law. Based on this law's properties, we describe in Section III the complementary law. In Section IV, we combine the two laws. Finally, in Section V we describe the experiments conducted on a real robotic platform.

II. Basic Control Law

In this section, the basic control law, implemented in the past on a mobile robot [1], will be described. The objective of the law is to use angular information to calculate a motion vector $\overrightarrow{M}$ that, when updated at infinitesimally small intervals, drives the robot to a pre-specified goal position.

A. Definitions

A *snapshot* of the workspace from a configuration $P \in (\mathbb{R}^2 \times S^1)$, corresponds both to the sequence of visible landmarks and the angles with which the landmarks are visible from P. The current and the goal position of the robot will be denoted as A and T, respectively. The corresponding snapshots will have the same name. The *angular separation* between two landmarks L_i and L_j at A corresponds to the angle $\theta_{ij} \in [0, 2\pi)$ between $\overrightarrow{AL_i}$ and $\overrightarrow{AL_j}$, measured in counterclockwise order. If the corresponding angle for position T is θ'_{ij}, then the *difference in angular separation* of two landmarks L_i and L_j between A and T is defined as $\Delta\theta_{ij} = \theta'_{ij} - \theta_{ij}$. The *bisector vectors* $\overrightarrow{\delta_{ij}}\ \forall\ i, j \in [1, n]$ are defined so that they have unit length, start from A and have the same direction as the bisector of θ_{ij}. The unit vector from A to T is denoted as $\overrightarrow{\tau}$.

B. Description of the Basic Control Law

To understand the basic control law, we will first consider the case of two landmarks L_i and L_j. Eventually, the proposed framework will be presented for the case of three landmarks. If $\Delta\theta_{ij}$ is positive, then the robot views the two landmarks from position T with a greater angle than from position A. The robot should move in a direction that increases the angle θ_{ij}. If $0 \leq \theta_{ij} \leq \pi$ and $\Delta\theta_{ij} \geq 0$, the robot should move closer to the landmarks. All directions that are in the interior of the angle between vectors $\overrightarrow{AL_i}$ and $\overrightarrow{AL_j}$ will move the robot to a new position with higher θ_{ij}. Vector $\overrightarrow{\delta_{ij}}$ has such a direction. When $\theta_{ij} \geq \pi$, the bisector vector $\overrightarrow{\delta_{ij}}$ is still a valid direction for increasing the angle θ_{ij}. When $\Delta\theta_{ij}$ is negative, the robot should follow the inverse of vector $\overrightarrow{\delta_{ij}}$. A motion vector that has the above properties and smooth magnitude over the entire plane is the following:

$$\overrightarrow{M_{ij}} = \begin{cases} \Delta\theta_{ij} \cdot \overrightarrow{\delta_{ij}}, & -\pi \leq \Delta\theta_{ij} \leq \pi \\ (2\pi - \Delta\theta_{ij}) \cdot \overrightarrow{\delta_{ij}}, & \Delta\theta_{ij} > \pi \\ (-2\pi - \Delta\theta_{ij}) \cdot \overrightarrow{\delta_{ij}}, & \Delta\theta_{ij} < -\pi. \end{cases} \quad (1)$$

From Euclidean geometry is known that when a moving point follows the bisector defined by an angle between two points, the trajectory of the moving point is a section of a hyperbolic curve. In this case, it is the section going through A of the hyperbola with the landmark points as the foci. The robot is guaranteed to reach the circular arc $(L_i T L_j)$ at the point of intersection with the hyperbolic section, such as point T' in Fig. 2. Position T cannot be identified on this arc since for every point on the arc, $\overrightarrow{M}$ becomes zero. Consequently, given only two landmarks, Eq.1 will not guide the robot to the goal. However, if another landmark, L_k, is introduced in the environment, then T is constrained to lie on two more circular arcs. If Eq. 1 is applied for each pair of landmarks L_i and L_j, then a partial vector $\overrightarrow{M_{ij}}$ is defined. By taking the vector sum the resultant vector $\overrightarrow{M}$ is produced. The aim is to minimize the difference in angular separation for every pair of landmarks simultaneously.

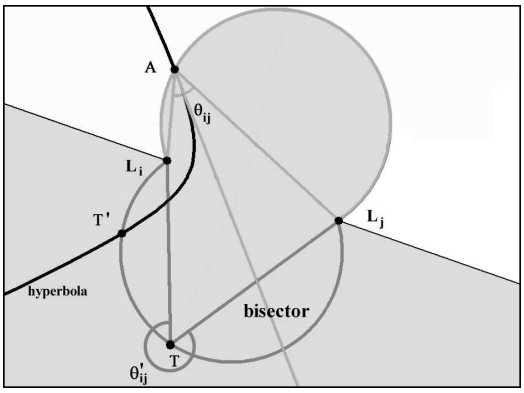

Fig. 2. When there are only two landmarks L_i and L_j available, the control law can only achieve the circular arc defi ned by the two landmarks and the goal position. In this case θ_{ij} is acute and $\Delta\theta_{ij}$ is positive.

Fig. 3 illustrates an example of how the component vectors and the resultant motion vectors are computed. $\overrightarrow{M_{ki}}$ and $\overrightarrow{M_{jk}}$ have the same direction as the bisectors $\overrightarrow{\delta_{ki}}$ and $\overrightarrow{\delta_{jk}}$, respectively. On the other hand, $\overrightarrow{M_{ij}}$ has

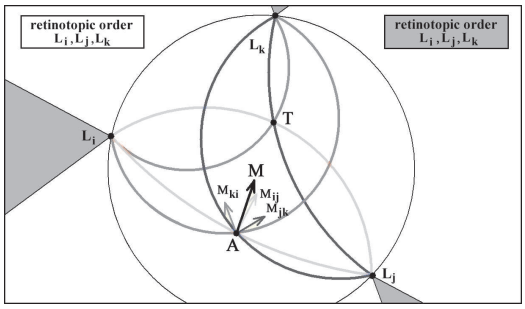

Fig. 3. An example of a scene with three landmarks L_i, L_j and L_k. The component vectors are computed using Eq. 1 and they are summed to produce $\vec{M}$.

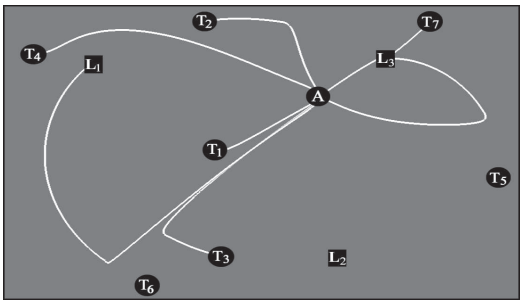

Fig. 4. Simulated paths when the robot follows $\vec{M}$ for various goal points. The control law fails to reach points T_6 and T_5.

opposite direction from $\overrightarrow{\delta_{ij}}$ because $\Delta\theta_{ij}$ is negative. But the magnitude of the difference $\Delta\theta_{ij}$ is the greatest, so $\overrightarrow{M_{ij}}$ will have the greatest magnitude. The control law can be summarized by the following equation:

$$\overrightarrow{M} = \overrightarrow{M_{ij}} + \overrightarrow{M_{jk}} + \overrightarrow{M_{ki}}, \quad (2)$$

where the component vectors are defined by Eq. 1. The robot can detect that it has reached the goal when $\forall\ i, j \in [1, 3] : \Delta\theta_{ij} = 0$ or for the actual implementation of the control law it is sufficient fro $\Delta\theta_{ij}$ to be less than a small predefined threshold.

C. Properties of the Basic Control Law

In this section, we present a new analysis of the control law's properties. This analysis is important for the construction of a system that reaches the entire plane.

1) Vector field and flow: For a particular goal position T and landmark configuration, Eq. 2, defines a vector field. When T is in the interior of the circumscribed circle of the landmarks, the vector field has a *sink* at point T (point T is a zero for the vector field). Fig. 4 shows simulated paths that have been produced with Eq. 2 for the same initial position A and seven different goal positions. Although the trace of the robot is not necessarily a straight line, if the robot adjusts its motion vector at every new position, it will converge to the goal in these cases. Points T_5 and T_6, however, were not successfully reached. For these points, the robot will first reach the circular arc defined by the goal and the two closest landmarks to it (e.g., landmarks L_1 and L_2 for position T_6) and then instead of moving closer to the goal it will follow the wrong direction on this arc and reach one of the landmarks.

2) Reachability: The *reachability set* of a system, for a given set of initial states A and a family of control inputs U is the set of goal states T that the system may be after time t [15]. The *backwards reachability set* (or catchment area [6]) is the set of states A that the system could be in before reaching the state T at time t. Although the analytic computation of reachable sets for discrete systems is a well understood problem, the computation of reachable sets for differential equations is much more challenging, especially for non-linear equations [10].

In order to determine the reachability set for the case of three landmarks, extensive experiments have been conducted on a simulator. Fig. 1(a) shows the result of an experiment where each pixel in the image is considered to be a possible goal configuration. This simulation aims at testing whether each point/pixel in the figure is a reachable goal position, if the robot starts from a specific position and senses the bearing angles of the depicted landmarks. The results after a series of simulations suggest that the reachability set of the basic control law for a scene with three landmarks that does not depend on the start position is the union of the following sets:

- The interior $\hat{C}$ of the circle defined by points L_1, L_2 and L_3.
- The union $\hat{H}$ of all sets H_j: A set H_j is the intersection of two half-planes. The first half-plane is defined by line (L_iL_j) and does not include landmark L_k, while the second is defined by the line L_jL_k and does not include landmark L_i, where $k \neq i \neq j \neq k$ (see Fig. 5).

From the above description of the reachability set, it is easy to conclude that *the backwards reachability set of the system for a goal state T in $\hat{C}$ or $\hat{H}$ will be the entire* $\mathbb{R}^2$. This is an important result, since previous homing algorithms were able to reach the goal only if the starting position was in the vicinity of the goal.

3) Dot product: Evaluating the dot product $(\overrightarrow{M} \cdot \overrightarrow{\tau})$, provides insight into why the reachability set of $\overrightarrow{M}$ is not the entire plane. If the angular separations do not differ a lot one with the other, then it can be shown that the dot product $(\overrightarrow{M} \cdot \overrightarrow{\tau})$ is positive for every possible goal. This property is related to the "isotropic landmark distribution" assumption [7]. In particular, an under-approximation of the set of points for which the dot product is positive is given by the following condition: *If at point A:* $\forall i, j, k : \frac{\theta jk}{2} \leq \theta_{ij} \leq 2 * \theta_{jk}$, *then the dot product* $(\overrightarrow{M'} \cdot \overrightarrow{\tau})$ *calculated at A is positive* $\forall\ T$.

When the robot's position is located outside the circle of the landmarks, there are neighboring points to A for which the dot product of every component motion vector is negative. We will define the π*-difference* of an angular separation θ_{ij} to be the following: $|\pi - \theta_{ij}|$. The *nearest landmark pair*

(NLP) to the goal is the pair of landmarks (L_iL_j), that has the minimum π-*difference*. The corresponding motion vector will be called the *nearest motion vector* (NMV).

From the study of the robot's path and the value of $(\overrightarrow{M} \cdot \overrightarrow{\tau})$ it can be shown that for an unreachable point T, the dominating component vector for the initial part of the robot's trajectory is the NMV. The robot follows a curve that is close to the hyperbola with the NLP landmarks L_i and L_j as the foci, until it approaches the circular arc (L_iTL_j). Close to the arc, the NMV stops dominating, because $\Delta\theta_{ij}$ approaches zero. Only if the goal position is located at the intersection of the curve and the arc (L_iTL_j) the robot reaches the goal. Otherwise, the robot reaches the arc and follows the opposite direction from the goal, because if A is on (L_iTL_j) and (L_i, L_j) is the NLP: $(\overrightarrow{M_{ij}} \cdot \overrightarrow{\tau}) = 0$ and $(\overrightarrow{M_{jk}} \cdot \overrightarrow{\tau}), (\overrightarrow{M_{ki}} \cdot \overrightarrow{\tau}) < 0$, consequently: $(\overrightarrow{M} \cdot \overrightarrow{\tau}) < 0$.

III. Complementary Control Law

The question that we are dealing with in this section is whether there exists a control law that uses only the bearing angles of landmarks and is capable of reaching the positions that are unreachable by the basic law. Our results are based on the study of the dot product $(\overrightarrow{M} \cdot \overrightarrow{\tau})$ and the simulated robot trajectories of the basic control law.

Algorithm 1 COMPLEMENTARY LAW(T)

Input: Snapshot T taken from the corresponding point.
Output: Motion vector.
repeat
  compute snapshot A, $nlp = (-1,-1)$, $mind_\pi$ = MAX_NUMBER
  for each pair of landmarks (i,j) **do**
    compute the difference $\Delta\theta_{ij} = \theta'_{ij} - \theta_{ij}$ and the vector $\overrightarrow{\delta_{ij}}$
    compute the π-difference: $d_\pi = |\theta'_{ij} - \pi|$
    use Eq. 1 to compute $\overrightarrow{M_{ij}}$
    if $d_\pi < mind_\pi$ **then**
      set $mind_\pi = d_\pi$ and $nlp = (i,j)$
    end if
  end for
  initialize $\overrightarrow{M}$ to the zero vector
  for each pair of landmarks (i,j) **do**
    if nlp is the pair (i,j) **then**
      add to $\overrightarrow{M}$ the vector: $\overrightarrow{M_{ij}}$ else add: $-\overrightarrow{M_{ij}}$
    end if
  end for
  the robot follows $\overrightarrow{M}$ for an infinitesimally small interval
until $\forall\ i,j \in [1,n] : \Delta\theta_{ij} = 0$

In particular, the robot can easily detect which landmark pairs do not correspond to the NLP. When the robot is close to the arc defined by the NLP, those two vectors guide the robot away from the goal. If the robot follows the opposite direction for these component vectors one should expect that points that were previously unreachable to become reachable. Algorithm 1 shows the complementary control law. Note that because the NLP depends only on the goal state, it can be computed once at the beginning of the path, and does not have to be recomputed at each iteration.

Fig. 5 shows that the reachability set for the new law is almost the complementary set of the reachability set of the basic control law that can be seen in Fig 1(a). The interior of the circle of the three landmarks and $\hat{H}$ are in general not reachable by the complementary law.

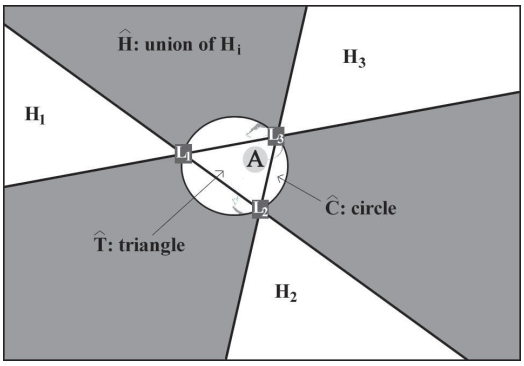

Fig. 5. The reachability set for the complementary law is depicted in gray color.

IV. Combining the proposed control laws

In this section we propose how to combine the two control laws that have complementary reachability areas in a single strategy with reachability area equal to the entire plane.

A. The Hybrid System

The solution to the combination of the laws can be given by building a finite automaton that decides which is the appropriate algorithm for a given goal. It is important to show that the decision regarding which algorithm to employ can be taken by considering only the bearing angles of three landmarks.

Fig. 6 shows the transition diagram and the states of the finite automaton. The states are the "basic uncertain" state, the "basic certain" state and the "complementary" one. The last two states are terminal states where the robot implements the corresponding algorithm. In the first state, however, the robot follows the basic control law and uses a set of rules in order to decide for a transition.

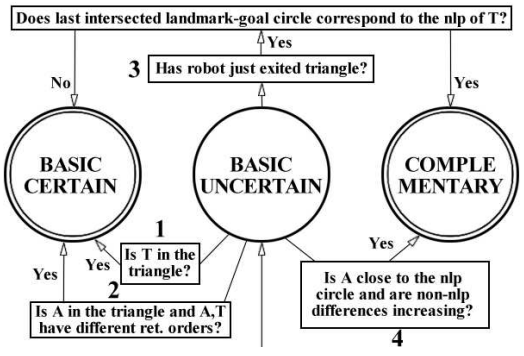

Fig. 6. The finite automaton that selects between the two control laws with complementary reachability sets.

Fig. 1(b) shows the reachability set of the resulting system. The circle defined by the three landmarks is the only set of points that is unreachable. This will always be true since every point on the circle has the same set of angular separations.

B. Description of the transitions

A set of definitions is necessary before describing the rules for the transitions between the states. For the following discussion, the interior of the triangle of the three landmarks will be $\hat{T}$. The circumscribed circle of T and two landmarks will be denoted as a landmark-goal circle. If the landmarks correspond to the NLP to the goal, then the corresponding circle will be the NLP landmark-goal circle. Let the retinotopic order of a point P to be the *cyclic string* of landmark identifiers for snapshots taken from P for all possible robot directions. In a three-landmark scene the plane can be divided into two sets of points with different retinotopic orders as Fig. 3 shows. The set $\hat{H}$ defines one of the two sets with different retinotopic orders. The transitions are now explained in the order given in Fig. 6.

1. Is T in $\hat{T}$? *The goal snapshot T is in the set $\hat{T}$ if and only if $\theta'_{ij} < \pi,\ \forall i, j \in [1, 3]$, where L_i and L_j are consecutive according to the retinotopic order.*

The first rule can be combined with the retinotopic property so as to distinguish goal positions in the set $\hat{H}$.

2. Is T in $\hat{H}$? *The goal snapshot T is in the set $\hat{H}$ if and only if T has different retinotopic order than A when A is in $\hat{T}$.*

Note that if the goal snapshot has been taken from the set $\hat{C} - \hat{T}$, it is impossible to determine based only on angular information from snapshot T, whether T has been taken from a position that is in $\hat{C}$. On the other hand, the robot is able to compute whether it intersects a landmark-goal circle. This requires just a comparison between the smallest angles in the sensor field of snapshots A and T created by the corresponding pair of landmarks. These angles are not the angular separations, they are defined so as to be in the interval $[0, \pi]$. If such an angle is wider in A, then the robot is inside the landmark-goal circle.

3. Is T in $\hat{C}$? *If A is in the opposite half-plane defined by the NLP to the goal from the one that T is in, but A is not in the interior of any landmark-goal circle and T is not in $\hat{T}$, the following statements are true if the basic control is applied: the robot is guaranteed to go through $\hat{T}$ and the last landmark-goal circle intersected before leaving $\hat{T}$ is the NLP circle, if and only if T is not in $\hat{C}$.*

The last criterion is related with the robot's perception of whether it approaches the goal or not.

4. Is T reachable? *The goal T is reachable by the basic control law if the non-NLP differences in angular separation decrease until they get to zero after the robot has reached the NLP landmark-goal circle.*

It is preferable when implementing the above criterion to start monitoring the non-NLP differences as soon as the NLP difference falls under a threshold. The previous criteria, are faster to detect whether one of the two algorithms is appropriate for a particular goal and produce smoother paths. The order with which these rules should be checked is the same with the order they are presented.

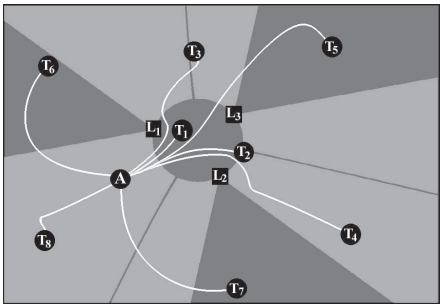

Fig. 7. Paths computed by the final system. In order to make the comparison easier, the reachability set of the initial algorithm is painted with dark gray color.

V. Experimental Validation

A series of experiments have been conducted in order to assess qualitatively and quantitatively the performance of the proposed angle-based navigation scheme. A simulator has been built which allows the design of 2D environments populated with landmarks and the visualization of paths. Examples of such paths as computed by the simulator can be seen in Fig. 7.

Another series of experiments employ an I-Robot, B21R robot equipped with a Neuronics, V-cam360 panoramic camera in a typical laboratory environment where three distinctive colored panels were used as landmarks. Landmarks were detected and tracked in the panoramic images acquired by the robot using a recently developed color-based tracker [2]. Fig. 8 shows a rough drawing of the robot's workspace where the sets $\hat{C}$, $\hat{H}$ are shown together with six marked positions. The size of the room was approximately 8m x 12m and the maximum speed that the robot was able to achieve was 0.30 m/sec translational speed and 0.1 rad/sec rotational speed. Note that these six positions cover every set of points that is important for the proposed algorithms, since $A \in \hat{T}$, $F \in \hat{C} - \hat{T}$, $C, D \in \hat{H}$ and B, E are positions in the rest of the plane.

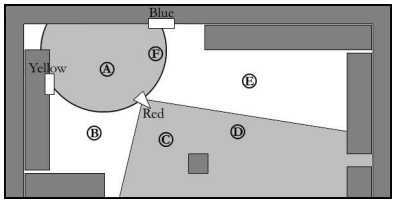

Fig. 8. The environment where the experiments were conducted.

The first navigation experiment was designed so as to provide evidence regarding the reachability sets in a real environment. Each algorithm has been tested for various start and goal positions and Table I shows the results of

running the hybrid system. The experiments have shown that the reachability sets of the basic control law and the complementary law are in agreement with simulation results. Furthermore, the hybrid control law reaches every goal position for which the path that the robot has to follow is obstacle-free and retains the visibility of landmarks. To further assess the accuracy of the hybrid system in reaching a goal position the hybrid algorithm was employed 30 times to reach each of the 6 marked positions in Fig. 8, resulting in 180 different runs. Table II summarizes the results of the experiments by providing the mean error and the standard deviation of the error in achieving each position. The accuracy in reaching a goal position is in the order of a few centimeters for all control laws.

Additional experiments have been carried out for different types of landmarks and different landmark configurations, including the special case of collinear landmarks. For example objects that already existed in the laboratory (e.g., doors, desks etc) had been used as landmarks. The algorithm was also successful in the case that a human was moving in the environment occasionally occluding the landmarks for a number of frames. The tracker was able to recapture the landmark as soon as it reappeared in the robot's visual field. In all the cases the accuracy in reaching the goal position was comparable to the results reported in tables I and II.

VI. Discussion

New algorithms have been developed that allow angle-based navigation to reach goal positions which were initially unreachable for a simple hill-climbing strategy, as Fig. 7 shows. With the addition of more landmarks in the scene the ambiguity on the circle of the landmarks can also be resolved. Another important issue is the behavior of the proposed framework under sensing uncertainty. Although experiments on a real robotic platform have been conducted and show good behavior, a study on the behavior of the algorithm under uncertainty would be interesting. The combinations of the proposed framework with other path planning techniques is the focus of current and future research.

TABLE I

Experiments for the reachability area of the combined law.

Algorithm		Hybrid Systems		
Experiment	Positions	A	C	E
1^{st}	Initial point	1.0 cm.	4.5 cm.	5.5 cm.
2^{nd}	somewhere in	2.0 cm.	3.5 cm.	8.5 cm.
3^{rd}	$\hat{C}$	4.0 cm.	3.0 cm.	3.0 cm.
1^{st}	Initial point	2.0 cm.	9.0 cm.	1.5 cm.
2^{nd}	somewhere in	3.5 cm.	3.0 cm.	6.5 cm.
3^{rd}	$\hat{H}$	2.0 cm.	3.0 cm.	3.5 cm.
1^{st}	Initial point	1.5 cm.	2.0 cm.	2.0 cm.
2^{nd}	not in $\hat{C}$	3.5 cm.	2.0 cm.	5.5 cm.
3^{rd}	or $\hat{H}$	1.5 cm.	3.5 cm.	8.0 cm.

TABLE II

Mean Error and Standard Deviation (Units: Centimeters)

Point:	A	B	E	D	F	C
Mean Er.	1.45	4.65	3.22	2.55	2.28	2.85
St. Dev.	1.13	2.10	1.96	1.35	1.22	1.41

Acknowledgments Work on this paper by K. Bekris and L. Kavraki has been partially supported by AMD, NSF 9702288, NSF 0308237 and a Sloan Fellowship to Lydia Kavraki.

References

[1] A. A. Argyros, K. E. Bekris, and S. E. Orphanoudakis. Robot Homing based on Corner Tracking in a Sequence of a Panoramic Images. In *CVPR*, volume 2, pages 3–10, Kauai, Hawaii, December 2001.

[2] A.A. Argyros and M.I.A. Lourakis. Real-time Tracking of Skin-colored Regions by a Potentially Moving Camera. In *Proc. of European Conference on Computer Vision (ECCV'04) - to appear*, Prague, Czech Republic, 2004.

[3] M. Betke and L. Gurvits. Mobile robot localization using landmarks. *IEEE Transactions on Robotics and Automation*, 13(2):251–263, 1997.

[4] K. Briechle and U. D. Hanebeck. Localization of a Mobile Robot Using Relative Bearing Measurements. 20(1):36–43, February 2004.

[5] B. A. Cartwright and T. S Collett. Landmark learning in bees: Experiments and models. *Computational Physiology*, 151:521–543, 1983.

[6] B. A. Cartwright and T. S Collett. Landmark maps for honeybees. *Biological Cybernetics*, 57:85–93, 1987.

[7] M. O. Franz, B. Scholkopf, H. A. Mallot, and H. H. Bulthoff. Where did I take that snapshot? Scene-based Homing by Image Matching. *Biological Cybernetics*, 79:191–202, 1998.

[8] B. Kuipers. The Spatial Semantic Hierarchy. *Artifi cial Intelligence*, 119:191–233, 2000.

[9] A. M. Ladd, K. E. Bekris, G. Marceau, A. Rudys, D. S. Wallach, and L. E. Kavraki. Using Wireless Ethernet for Localization. In *IROS*, Lausanne, Switzerland, October 2002.

[10] G. Lafferriere, G. J. Pappas, and S. Yovine. Symbolic Reachability Computation for Families of Linear Vector Fields. *Journal of Symbolic Computation*, 11, 2001.

[11] D. Lambrinos, R. Moller, T. Labhart, R. Pfeifer, and R. Wehner. A mobile robot employing insect strategies for navigation. *Robotics and Autonomous Systems*, 30:39–64, 2000.

[12] S. Lenser and M. Veloso. Visual sonar: Fast Obstacle Avoidance using Monocular Vision. In *Proc. of the IEEE/RSJ IROS 2003*, Las Vegas, NV, October 2003.

[13] T. S. Levitt and D. T. Lawton. Qualitative Navigation for Mobile Robots. *Artifi cial Intelligence*, 44:305–360, 1990.

[14] L. M. Lorigo, R. A. Brooks, and W. E. L. Grimson. Visually-Guided Obstacle Avoidance in Unstructured Environments. In *Proc. of the IEEE/RSJ IROS 1997*, pages 373–379, 1997.

[15] I. M. Mitchell. *Application of Level Set Methods to Control and Reachability Problems in Continuous and Hybrid Systems*. PhD thesis, Stanford University, August 2002.

[16] R. Moller. Insect Visual Homing Strategies in a robot with Analog Processing. *Biological Cybernetics, special issue: Navigation in Biological and Artifi cial Systems*, 83-3:231–243, 2000.

[17] M. Montemerlo, S. Thrun, D. Koller, and B. Wegbreit. FastSLAM: A Factored Solution to the Simultaneous Localization and Mapping Problem. In *Proc. of the AAAI National Conference on Artifi cial Intelligence*, Edmonton, Canada, 2002. AAAI.

[18] D. Niculescu and B. Nath. Ad Hoc Positioning System (APS) using Angle of Arrival (AoA). In *IEEE INFOCOM*, San Francisco, CA, 2003.

[19] E. Remolina and B Kuipers. Towards a general theory of topological maps. *Artifi cial Intelligence*, 152:47–104, 2004.

[20] S. Thrun. Probabilistic Algorithms in Robotics. *AI Magazine*, 21(4):93–109, 2000.

[21] I. Ulrich and J. Borenstein. VFH*: Local Obstacle Avoidance with Look-ahead Verifi cation. In *Proc. of the 2000 IEEE International Conference on Robotics and Automation*, pages 2505–2511, San Fransisco, CA, April 2000.